Article

C-Labeled *N*-Acetyl-neuraminic Acid in Aqueous Solution: Detection and Quantification of Acyclic Keto, Keto Hydrate, and Enol Forms by C NMR Spectroscopy

Thomas Klepach, Ian Carmichael, and Anthony S. Serianni

J. Am. Chem. Soc., **2008**, 130 (36), 11892-11900 • DOI: 10.1021/ja077565g • Publication Date (Web): 19 August 2008

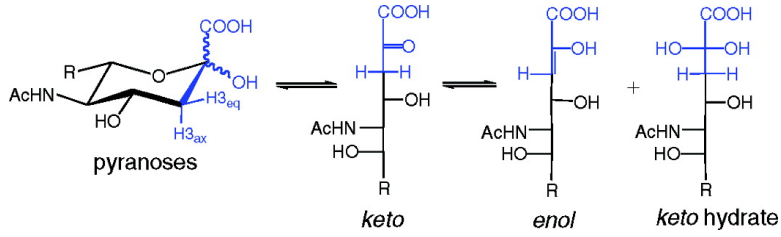

More About This Article

Additional resources and features associated with this article are available within the HTML version:

- Supporting Information
- Access to high resolution figures
- Links to articles and content related to this article
- Copyright permission to reproduce figures and/or text from this article

View the Full Text HTML

J|A|C|S
ARTICLES

Published on Web 08/19/2008

^{13}C-Labeled *N*-Acetyl-neuraminic Acid in Aqueous Solution: Detection and Quantification of Acyclic Keto, Keto Hydrate, and Enol Forms by ^{13}C NMR Spectroscopy

Thomas Klepach,[†] Ian Carmichael,[‡] and Anthony S. Serianni*,[†]

Department of Chemistry and Biochemistry and the Radiation Laboratory, University of Notre Dame, Notre Dame, Indiana 46556-4670

Received October 5, 2007; E-mail: aseriann@nd.edu

Abstract: Aqueous solutions of *N*-acetyl-neuraminic acid (Neu5Ac, **1**) labeled with ^{13}C at C1, C2, and/or C3 were analyzed by ^{13}C NMR spectroscopy to detect and quantitfy the acyclic forms (keto, keto hydrate, enol) present at varying pHs. In addition to pyranoses, solutions contained the keto form, based on the detection of C2 signals at ~198 ppm (~0.7% at pH 2). Spectra of [2-^{13}C] and [3-^{13}C] isotopomers contained signals arising from labeled carbons at ~143 and ~120 ppm, respectively, which were attributed to enol forms. Solution studies of [1,2,3-$^{13}C_3$]**1** substantiated the presence of enol (~0.5% at pH 2). Enol was not detected at pH > 6.0. A C2 signal observed at ~94 ppm was identified as C2 of the keto hydrate (~1.9% at pH 2), based partly on its abundance as a function of solution pH. Density functional theory (DFT) calculations were used to study the effect of enol and hydrate structure on J_{CH} and J_{CC} values involving C2 and C3 of these forms. Solvated DFT calculations showed that $^2J_{C2,H3}$ in *cis* and *trans* enols have similar magnitudes but opposite signs, making this *J*-coupling potentially useful to distinguish enol configurations. Solvent deuterium exchange studies of **1** showed rapid incorporation of ^{2}H from ^2H_2O at H3$_{axial}$ in the pyranoses at p^{2}H 8.0, followed by slower exchange at H3$_{equatorial}$. The acyclic keto form, which presumably participates in this reaction, must assume a pseudo-cyclic conformation in solution in order to account for the exchange selectivity. Weak ^{13}C signals arising from labeled species were also observed consistently and reproducibly in aqueous solutions of ^{13}C-labeled **1**, possibly arising from products of lactonization or intermolecular esterification.

Introduction

N-Acetyl-neuraminic acid (Neu5Ac, **1**, Scheme 1) is a C_9 α-ketoacid often encountered as the terminal residue of complex-type *N*-glycans covalently bound to human glycoproteins such as immunoglobulin G (IgG).[1,2] Neu5Ac is commonly installed on glycoproteins and glycolipids in 2→3 or 2→6 linkage with terminal *β*-Gal residues via the involvement of the biologically activated Neu5Ac donor, CMP-*N*-acetyl-neuraminic acid (CMP-Neu5Ac), and CMP-Neu5Ac sialyltransferase (EC 2.4.99.1, 2.4.99.4).[3] The presence of Neu5Ac on glycoproteins has been shown to influence their biological functions. For instance, the anti- and pro-inflammatory activities of human IgG have been shown to correlate with the presence and absence of Neu5Ac, respectively, on the Fc fragment.[4] Neu5Ac is derived from C_6 and C_3 metabolites *in vivo*, although the specific forms of these building blocks depend on the organism. In *Escherichia coli*, Neu5Ac is produced from *N*-acetyl-D-mannosamine (ManNAc) and pyruvate in an aldol condensation reaction catalyzed by *N*-acetyl-neuraminate lyase (EC 4.1.3.3).[5] In other organisms, ManNAc or ManNAc-6P and phosphoenolpyruvate (PEP) are substrates for sialic acid synthases, yielding Neu5Ac or Neu5Ac-9P, respectively.[6]

Scheme 1. Anomerization of Neu5Ac (**1**) and Abundances of Forms in Aqueous Solution at pH 2.0

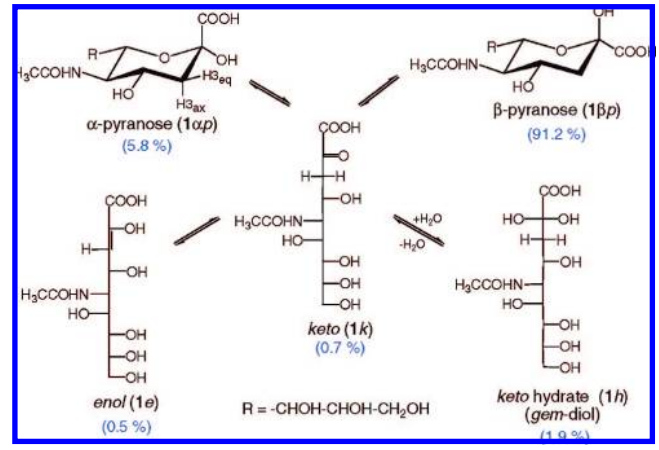

Studies in this laboratory of the conformational and dynamic properties of biologically important oligosaccharides containing

[†] Department of Chemistry and Biochemistry.
[‡] Radiation Laboratory.

(1) Dwek, R. A.; Lellouch, A. C.; Wormald, M. R. *J. Anat.* **1995**, *187*, 279–292.
(2) Wormald, M. R.; Rudd, P. M.; Harvey, D. J.; Chang, S.-C.; Scragg, I. G.; Dwek, R. A. *Biochemistry* **1997**, *36*, 1370–1380.
(3) Breton, C.; Snajdrova, L.; Jeanneau, C.; Koca, J.; Imberty, A. *Glycobiology* **2006**, *16*, 29R–37R.
(4) Kaneko, Y.; Nimmerjahn, F.; Ravetch, J. V. *Science* **2006**, *313*, 670–673.
(5) Maru, I.; Ohnishi, J.; Ohta, Y.; Tsukada, Y. *J. Biosci. Bioeng.* **2002**, *93*, 258–265.
(6) Tanner, M. E. *Bioorg. Chem.* **2005**, *33*, 216–228.

10.1021/ja077565g CCC: $40.75

Neu5Ac glycosidic linkages required **1** containing specific sites of ^{13}C-enrichment to allow measurements of NMR parameters such as trans-glycoside J_{CH} and J_{CC} spin−spin coupling constants. The availability of Neu5Ac singly labeled with ^{13}C at C1, C2, and C3 stimulated tangential ^{13}C NMR investigations of the solution composition of **1**. Prior work has shown that selective ^{13}C-labeling at the anomeric carbons of aldoses and ketoses allows the detection and quantification not only of major tautomeric forms in solution, which are often cyclic, but also of acyclic forms (aldehydo and keto forms and their hydrates), which are normally present in very low abundance.[7–9] Knowledge of the solution behavior of **1** contributes to a better understanding of its biological properties, especially with respect to identifying potential monomeric forms bound by Neu5Ac-recognizing enzymes and receptors. We describe herein ^{13}C NMR studies of aqueous solutions of Neu5Ac ^{13}C-isotopomers and show that these solutions contain detectable amounts of acyclic keto, keto hydrate, and enol forms.

Experimental Section

A. ^{13}C-Labeled Neu5Ac. [1-^{13}C]-, [2-^{13}C]-, [3-^{13}C]-, and [1,2,3-$^{13}C_3$]Neu5Ac isotopomers were obtained from Omicron Biochemicals, Inc. (South Bend, IN) and used without further purification.

B. Preparation of Unlabeled Neu5Ac. Unlabeled **1** was prepared by a modification of the procedure described by Czarniecki and Thornton.[10] Two batches of edible bird's nest (batch A, 27.7 g; batch B, 28.1 g), obtained from Hsu's Ginseng Enterprises, Inc. (http://english.hsuginseng.com), were each homogenized in 50 mL of distilled H_2O using a Waring blender. The homogenate was diluted to a final volume of 3 L containing H_2SO_4 at a concentration of ∼0.025 M. The solution was stirred at 60−70 °C for 2.5 h. A saturated aqueous solution of $Ba(OH)_2$ was then added slowly to the mixture until the pH was between 5 and 6. The mixture was incubated at 4 °C overnight and then vacuum filtered through a glass microfiber filter. The clear filtrate was concentrated *in vacuo* to ∼250 mL and passed through a 0.3 μm filter, which was washed with water after the filtration. The combined filtrate and washings were split into two equal volumes (∼130 mL each) and individually loaded onto a Dowex 1 × 8 (200−400 mesh) ion-exchange column (3.0 × 30.0 cm) in the formate form. After loading, the column was washed with 1 L of distilled water and then eluted with a 1.5 L linear formic acid gradient (0−2 M). Fractions (23 mL) were collected and assayed by spotting fraction aliquots on silica gel thin layer chromatography (TLC) plates, spraying with molybdate reagent (1% (w/v) $CeSO_4$−2.5% (w/v) $(NH_4)_6Mo_7O_{24}$−10% aq H_2SO_4),[11] and charring. Fractions testing positive for Neu5Ac were combined, and the resulting solution was lyophilized. Total yield of Neu5Ac: ∼1.7 g each from batches A and B. The white powder had a melting point of 184−186 °C and was found to be >98% pure by 1D ^{1}H and ^{13}C NMR analyses.

C. Preparation of 2-*O*-Methyl-β-D-*N*-acetyl-neuraminic Acid (2).[10] Unlabeled **1** (100 mg, 0.32 mmol) was dissolved in 80 mL of dry methanol, 3 g of Dowex 50 × 8 (200−400 mesh) ion-exchange resin in the H^+ form was added, and the suspension was refluxed at 76 °C. The reaction was monitored by silica gel TLC (butanol:acetic acid:H_2O, 2:1:1) using molybdate reagent for visualization[11] (see above). The reaction was stopped after 48 h, cooled, and filtered to remove the resin, and the filtrate was concentrated *in vacuo* to give ∼85 mg of crude syrup. 1D ^{1}H and ^{13}C NMR analysis showed that methyl 2-*O*-methyl-β-D-*N*-acetyl-neuraminate methyl ester was the primary product. ^{13}C NMR: δ 171.81 (C1); 100.60 (C2); 40.61 (C3); 67.82, 53.11, 71.93, 69.41, 71.24, 64.77 (C4−C9); 176.21 (acetyl CO); 23.48 (acetyl CH_3); 52.40 (glycoside CH_3); 54.94 (ester CH_3).

The methyl ester was saponified for 12 h in 1 M NaOH, after which the solution pH was lowered to ∼1.4 with the addition of Dowex (H^+) ion-exchange resin. 1D ^{1}H and ^{13}C NMR analyses showed conversion to the free acid methyl glycoside **2**. ^{13}C NMR: δ 171.46 (C1); 95.40 (C2); 38.74 (C3); 66.72, 52.13, 70.40, 68.26, 70.15, 63.22 (C4−C9); 174.86 (acetyl CO); 22.15 (acetyl CH_3); 53.56 (ester CH_3).

D. NMR Spectroscopy. Solutions (∼300 μL, ∼0.1 M) of ^{13}C-labeled compounds in 95:5 v/v ^1H_2O:^2H_2O solvent were prepared and transferred to 3-mm NMR tubes. Quantitative 1D $^{13}C\{^1H\}$ NMR spectra were obtained at 25 °C on a Varian UnityPlus 600-MHz FT-NMR spectrometer operating at 150.856 MHz for ^{13}C and equipped with a 3-mm $^{13}C/^1H$ microprobe (Nalorac).

For non-quantitative measurements, $^{13}C\{^1H\}$ NMR spectra were typically obtained with a 36 496 Hz spectral window and 27.75 s recycle time (^{13}C T_1's were not longer than ∼5 s under the experimental solution conditions, as determined from τ_{null} values in an inversion−recovery T_1 experiment). Free induction decays (FIDs) were zero-filled once or twice to give final digital resolutions of <0.05 Hz/pt, and FIDs were processed with resolution enhancement (Gaussian or sine-bell functions) to improve resolution and facilitate the measurement of small *J*-couplings. The degree of enhancement was chosen empirically on the basis of the observed spectral S/N and quality.

For quantitative measurements, ^{13}C NMR spectra were collected with ^{1}H-decoupling during FID acquisition and without nuclear Overhauser enhancement (NOE) buildup during the interpulse delays (35 s) to allow for more reliable determinations of the percentage of the different forms in solution. A minimal line-broadening window function was applied prior to signal integration.

Calculations

A. Selection and Geometric Optimization of Model Compounds. Structures **3** and **4**−**7** were chosen as mimics of **1***h* and **1***e*, respectively. Solvated density functional theory (DFT) calculations were conducted within *Gaussian*03[12] using the B3LYP functional[13] and 6-31G* basis set[14] for geometric optimization, as described previously.[15,16] Initial torsion angle constraints in **3** were as follows: C2−C3−C4−C5 torsion fixed at −165°; C3−C2−O2−H, C3−C2−O2′−H, C3−C4−O4−H, and C2−C1−O1′−H torsions fixed at 180°; O1−C1−C2−C3 torsion set initially at 90° and allowed to optimize. For **4** and **5**, the C3−C4−O4−H, C2−C1−O1−H, and C3−C2−O2−H torsions were fixed at 180°. For **6** and **7**, the C3−C4−O4−H, C3−C2−O2−H, and C2−C1−O1′−H torsions were fixed at 180°. The C1−C2−C3−C4 torsion angle was fixed at 0° in **4** and **6** (*cis* enols) and at 180° in **5** and **7** (*trans* enols). Two orientations of the COOH group in **4** and **5** were examined in which the double bonds were conjugated (O1′−C1−C2−C3 torsion fixed at 180°) and unconjugated (O1′−C1−C2−C3 torsion was fixed at 90°). In **6** and **7**, the C2−C3−C4−C5 torsion angle was rotated in 30° increments from 90° to 270° in two O1′−C1−C2−C3 rotamers (90° and 180°). All remaining geometric parameters were optimized except those identified above.

(7) Maple, S. R.; Allerhand, A. *J. Am. Chem. Soc.* **1987**, *109*, 3168–3169.
(8) Drew, K. N.; Zajicek, J.; Bondo, G.; Bose, B.; Serianni, A. S. *Carbohydr. Res.* **1998**, *307*, 199–209.
(9) Zhu, Y.; Zajicek, J.; Serianni, A. S. *J. Org. Chem.* **2001**, *66*, 6244–6251.
(10) Czarniecki, M. F.; Thornton, E. R. *J. Am. Chem. Soc.* **1977**, *99*, 8273–8279.
(11) Tropper, F. D.; Andersson, F. O.; Grand-Maitre, C.; Roy, R. *Carbohydr. Res.* **1992**, *229*, 149–154.
(12) Frisch, M. J.; *et al. Gaussian03*, Revision A.1; Gaussian, Inc., Pittsburgh, PA, 2003.
(13) Becke, A. D. *J. Chem. Phys.* **1993**, *98*, 5648–5652.
(14) Hehre, W. J.; Ditchfield, R.; Pople, J. A. *J. Chem. Phys.* **1972**, *56*, 2257–2261.
(15) Cloran, F.; Zhu, Y.; Osborn, J.; Carmichael, I.; Serianni, A. S. *J. Am. Chem. Soc.* **2000**, *122*, 6435–6448.
(16) Cloran, F.; Carmichael, I.; Serianni, A. S. *J. Am. Chem. Soc.* **2001**, *123*, 4781–4791.

B. DFT Calculations of $^{13}C-^{1}H$ and $^{13}C-^{13}C$ Spin-Coupling Constants. J_{CH} and J_{CC} values were calculated in **3**−**7** with *Gaussian*03[12] using DFT (B3LYP).[13] Couplings were calculated using the previously reported [5s2p1d|3s1p] basis set,[17] and raw (unscaled) calculated couplings are reported.

For all calculated geometries and *J*-couplings, the effect of solvent water was included by using the Self-Consistent Reaction Field (SCRF)[18] and the Integral Equation Formalism (polarizable continuum) model (IEFPCM)[19] as implemented in *Gaussian*03.[12]

Results and Discussion

A. Cyclic Pyranose and Acyclic Keto Forms of 1. Neu5Ac labeled with ^{13}C at the anomeric (C2) carbon was used to detect and quantify monomeric forms present in aqueous solution (Scheme 1). The $^{13}C\{^{1}H\}$ NMR spectrum of [2-^{13}C]**1** at pH 2.0 contained intense signals arising from labeled carbons in the α-pyranose (**1**α*p*, 96.53 ppm) and *β*-pyranose (**1**β*p*, 95.97 ppm)[20,21] forms (Figure 1A). The *β*-pyranose was significantly more abundant (91.2%) than the α-pyranose (5.8%) at pH 2.0; these percentages were 92.1% and 7.5%, respectively, at pH 8.0. The preference for the *β*-pyranose presumably derives from the anomeric effect,[22–24] which favors an axial C2−O2 bond, and from the greater steric demand of the COOH group relative to OH, which favors an equatorial C1−C2 bond. Both effects are reinforcing. The α*p*/β*p* ratio at pH 2.0 (0.064) was slightly smaller than the same ratio at pH 8.0 (0.081).

The $^{13}C\{^{1}H\}$ NMR spectrum of [2-^{13}C]**1** at pH 2.0 also contained a relatively intense signal at 198.20 ppm (Figure 1B), which was attributed to C2 of the acyclic keto (carbonyl) form (**1***k*). This signal appeared farther upfield than observed previously for the acyclic keto forms of D-[2-^{13}C]ribulose-5P (213.7 ppm),[25] D-[2-^{13}C]ribulose-1,5-bisphosphate (211.7 ppm),[25] and the D-[2-^{13}C]pentuloses (∼214 ppm)[26] and probably reflects the effect of C1 structure on δ_{C2} (COOH vs CH_2OH/CH_2OP). Integration of the spectrum acquired at pH 2.0 and 25 °C indicated that **1***k* comprises ∼0.7% of the total forms in solution; this percentage decreased to ∼0.4% at pH 8.0. At pH 2.0, an α*p*:β*p*:keto ratio of 8:130:1 was observed, whereas at pH 8.0, the ratio was 19:230:1.

B. Acyclic Hydrate Form of 1. The anomeric region of the $^{13}C\{^{1}H\}$ NMR spectrum of [2-^{13}C]**1** at pH 2.0 contained two relatively strong signals arising from labeled carbons at 95.90 and 93.60 ppm (Figure 1A, signals denoted X_1 and X_2, respectively). These chemical shifts are consistent with those

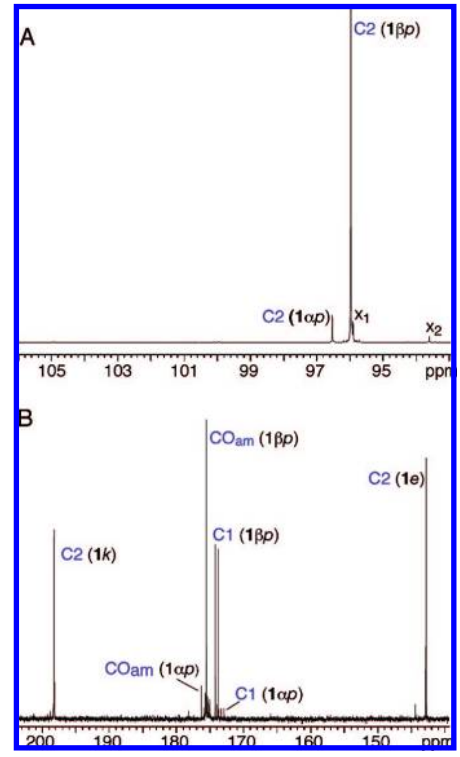

Figure 1. Partial $^{13}C\{^{1}H\}$ NMR spectrum of [2-^{13}C]**1** (150 MHz) at pH 2.0 and 25 °C showing signal assignments. (A) Anomeric region. X_1 and X_2 are putative C2 signals of the acyclic hydrate form (1*h*). (B) Region containing the labeled C2 keto (1*k*) and enol (1*e*) carbons, and the natural abundance amide CO (CO_{am}) and C1 (COOH) carbons of **1**β*p* and **1**β*p*. The C1 signals appear as doublets due to the presence of $^{1}J_{C1,C2}$. Several weak signals in this region were not identified.

expected for the acyclic keto hydrate form, **1***h*.[25] The X_2 signal was assigned tentatively to C2 of **1***h* on the basis of its relative abundance (1.9%) and the observed keto hydrate/keto ratio of ∼2.7, which is comparable to the corresponding ratio for pyruvic acid (2.31 ± 0.02).[27] By comparison, 2-ketose phosphates give keto hydrate/keto ratios of <1 (e.g., 0.14 for D-ribulose-1,5-bisphosphate; δ_{C2} 97.6 ppm), while no keto hydrate form was detected in ^{13}C NMR spectra of aqueous solutions of the D-[2-^{13}C]2-pentuloses.[25,26]

Since $C2_{\mathbf{1}h}$ is unprotonated, experimental support for its assignment could not be obtained by examining the magnitude of $^{1}J_{CH}$, which has been used previously to identify hydrate C1 carbons in aqueous solutions of [1-^{13}C]aldoses.[8,9] Therefore, two alternative assignment strategies were investigated.

Previous studies have shown that pyruvate anion is much less extensively hydrated than pyruvic acid in aqueous solution (keto hydrate/keto ratios in the anion range from 0.054 to 0.087).[27–30] This behavior was confirmed by inspection of ^{13}C NMR spectra of pyruvic acid and sodium pyruvate (Figure S1). By analogy to pyruvate, the intensity of the authentic $C2_{\mathbf{1}h}$ signal should decrease significantly upon raising the solution pH from 2.0 to 7.0. Titration of a solution of [2-^{13}C]**1** at pH 2.0 with NaOH

(17) Stenutz, R.; Carmichael, I.; Widmalm, G.; Serianni, A. S. *J. Org. Chem.* **2002**, *67*, 949–958.
(18) Cancés, M. T.; Mennucci, B.; Tomasi, J. *J. Chem. Phys.* **1997**, *107*, 3032.
(19) Cammi, R.; Mennucci, B.; Tomasi, J. *J. Phys. Chem. A* **2000**, *104*, 5631.
(20) The chemical shift of $C2_{\mathbf{1}\beta p}$ (free acid) was assigned as described previously (Gervay, J.; Batta, G., *Tetrahedron Lett.* **1994**, *35*, 3009–3012) using internal dioxane (δ 67.4 ppm) as the reference. All ^{13}C NMR spectra of **1** at pH 2 were referenced in this fashion.
(21) Assignments of the anomeric distribution of the pyranose forms of **1** and related structures have been reported previously from analyses of $^{3}J_{C1,H3ax}$ and $^{3}J_{C1,H3eq}$ couplings: Czarniecki, M.; Thornton, E. R. *J. Am. Chem. Soc.* **1977**, *99*, 8273–8279; Hori, H.; Nakajima, T.; Nishida, Y.; Ohrui, H.; Meguro, H. *Tetrahedron Lett.* **1988**, *29*, 6317–6320; Májer, G.; Borbás, A.; Illyés, T. Z.; Szilágyi, L.; Bényei, A. C.; Lipták, A. *Carbohydr. Res.* **2007**, *342*, 1393–1404.
(22) Edward, J. T. *Chem. Ind.* **1955**, 1102.
(23) Lemieux, R. U. In *Molecular Rearrangements*; de Mayo, P., Ed.; Interscience Publishers: New York, 1964; p 709.
(24) Juaristi, E.; Cuevas, G. *The Anomeric Effect*; CRC Press: Boca Raton, FL, 1995.
(25) Serianni, A. S.; Pierce, J.; Barker, R. *Biochemistry* **1979**, *18*, 1192–1199.
(26) Vuorinen, T.; Serianni, A. S. *Carbohydr. Res.* **1990**, *209*, 13–31.
(27) Chiang, Y.; Kresge, A. J.; Pruszynski, P. *J. Am. Chem. Soc.* **1992**, *114*, 3103–3107.
(28) Greenzaid, P.; Luz, Z.; Samuel, D. *J. Am. Chem. Soc.* **1967**, *89*, 749–756.
(29) Pocker, Y.; Meany, J. E.; Nist, B. J.; Zadorojny, C. *J. Phys. Chem.* **1969**, *73*, 2872–2882.
(30) Cooper, A. J. L.; Redfield, A. G. *J. Biol. Chem.* **1975**, *250*, 527–532.

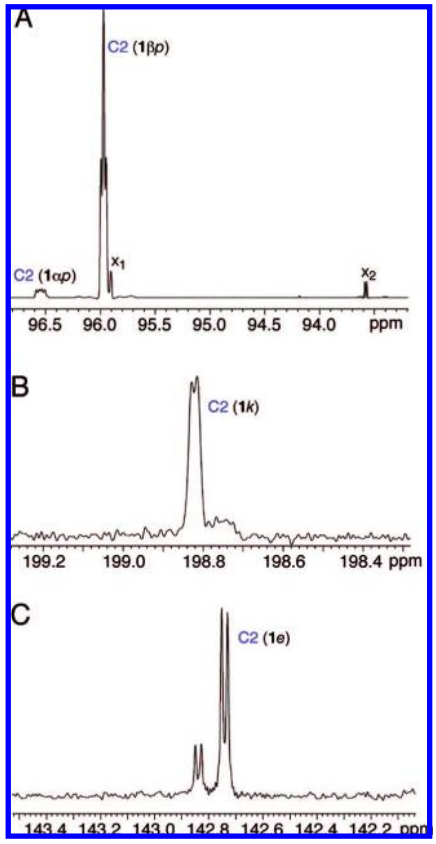

Figure 2. Partial ^{1}H-coupled ^{13}C NMR spectrum (150 MHz) of [2-^{13}C]**1** at pH 2.0 and 25 °C. (A) C2 signals of **1**α*p*, **1**β*p*, X_1, and X_2. (B) The C2 keto signal. (C) The C2 enol signals.

resulted in the disappearance of signals X_1 and X_2 at pH ∼6−7, but only X_2 reappeared at 93.60 ppm upon lowering the pH of the same solution back to 2.0 with HCl. These results suggest that X_2 is the correct $C2_{\mathbf{1}h}$ carbon signal.

A second approach to assign the $C2_{\mathbf{1}h}$ signal involved an interpretation of the X_1 and X_2 signal multiplicities observed in the ^{1}H-coupled ^{13}C NMR spectrum of [2-^{13}C]**1**. The multiplicities of the C2 signals of **1**α*p* and **1**β*p* (Figure 2A) served as internal controls. The $C2_{\mathbf{1}\alpha p}$ signal appeared as a doublet of doublets with J_{CH} values of ∼3.9 and ∼7.5 Hz, whereas the $C2_{\mathbf{1}\beta p}$ signal appeared as a pseudo-triplet containing J_{CH} values of ∼3.5 Hz. These couplings were consistent with the more accurate $^2J_{C2,H3ax}$ and $^2J_{C2,H3eq}$ values measured directly from the ^{1}H NMR spectrum of [2-^{13}C]**1**.[31] $^3J_{C2,H4}$ and $^3J_{C2,H6}$ values in **1**α*p* and **1**β*p* are associated with C2−C3−C4−H4 and C2−O6−C6−H6 torsion angles of ∼ −60° and ∼60°, respectively, and thus their small magnitudes appear as line-broadening in the ^{13}C multiplets. Signal X_1 appeared broadened, whereas X_2 appeared as a doublet with a splitting of ∼2.9 Hz (Figure 2A). By comparison, the $C2_{\mathbf{1}k}$ signal appeared as a broadened doublet with a splitting of ∼2.1 Hz (Figure 2B).

An inspection of molecular models of **1***h* showed that, in geometries having C2 *anti* to H4, destabilizing 1,3-interactions exist between the substituents at C2 and C4 that are likely to destabilize this conformation. Conformations having C2 and H4 *gauche* would yield a small $^3J_{C2,H4}$, undetectable in the ^{1}H-coupled ^{13}C NMR spectrum (the conformation having C2 *anti* to C5 appears more stable). Thus, non-zero J_{CH} values involving $C2_{\mathbf{1}h}$ are predicted to involve only the geminal C3 protons. If the signal at 93.60 ppm (X_2) is $C2_{\mathbf{1}h}$, then one putative $^2J_{CH}$ is ∼2.9 Hz, and the other is small or zero. Application of the projection rule[32] to the three staggered C2−C3 rotamers of **1***h* predicted small or 0 Hz values for both $^2J_{CH}$'s in one rotamer (that having C1 *anti* to C4), whereas the remaining two rotamers yielded a small or 0 Hz coupling to one H3 and a negative coupling to the other (Scheme S2). Thus, the observation of a single non-zero $^2J_{CH}$ is consistent with **1***h* having C2 *anti* to C5, and C1 *gauche* to C4 (either latter *gauche* conformation appears consistent with the experimental couplings). The second putative $C2_{\mathbf{1}h}$ signal, X_1, showed small or zero $^2J_{CH}$ values, consistent with **1***h* having C2 *anti* to C5, and C1 *anti* to C4.

Solvated DFT calculations on Neu5Ac hydrate mimic **3** were conducted to evaluate the effect of C2−C3 bond rotation on calculated $^2J_{C2,H3R/S}$ values and total energies. In these calcula-

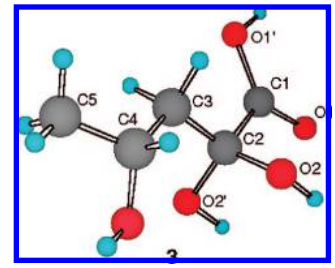

tions, the C2−C3−C4−C5 torsion angle was fixed at −165°, which gave calculated $^3J_{C2,H4}$ values of ∼0.6 Hz that are consistent with the NMR results. This treatment assumes that the small experimental $^3J_{C2,H4}$ correlates with a relatively rigid C2−C3−C4−H4 torsion angle of ∼75° in solution. Conformations of **3** containing C1−C2−C3−C4 torsion angles of 60° and −60° were found to be lower in energy than that containing a torsion angle of 180° (Figure S2A), favoring assignment of the hydrate C2 signal to X_2. However, calculated $^2J_{C2,H3R/S}$ couplings show that, for torsions near 90°, one coupling is ∼ −1.5 Hz and the other ∼ −7.5 Hz. These results are in modest agreement with experiment (∼0 and ∼ ±2.9 Hz) for X_2. Other conformational variables not investigated here (e.g., conformation about the C1−C2 bond) may contribute to the discrepancy.

$^1J_{C1,C2}$ and $^1J_{C2,C3}$ values were also computed in **3** as a function of the C2−C3−C4−C5 torsion angle (Figure S2B). Both couplings are relatively insensitive to the C2−C3 bond torsion, with the former considerably larger than the latter. The calculated couplings are in reasonable agreement with those observed experimentally for X_2 ($^1J_{C1,C2}$ = 69.5 Hz; $^1J_{C2,C3}$ = 44.0 Hz).

C. Acyclic Enol Forms of 1. The ^{13}C{^{1}H} NMR spectrum of [2-^{13}C]**1** contained relatively strong signals associated with labeled carbons at 142.75 and 142.85 ppm (Figure 1B). Signals in this spectral region commonly arise from unsaturated carbons. Possible candidates are enol forms **1***e* (Scheme 1) in *cis* and *trans* configurations (Scheme 2). An additional small signal was also observed at 144.39 ppm (Figure 1B). Integration of these three signals at pH 2.0 gave a total abundance of ∼0.5%.

Experimental support for the presence of **1***e* was obtained from the ^{13}C{^{1}H} NMR spectrum of [3-^{13}C]**1**. This spectrum

(31) ^{1}H NMR data showed significantly different (absolute) $^2J_{C2,H3ax}$ and $^2J_{C2,H3eq}$ values in **1**α*p* (7.7 and 4.3 Hz, respectively), whereas nearly identical couplings were observed in **1**β*p* (∼3.6 Hz). As reported previously for $^3J_{C1,H3ax}$ and $^3J_{C1,H3eq}$ (Hori, H.; Nakajima, T.; Nishida, Y.; Ohrui, H.; Meguro, H. *Tetrahedron Lett.* **1988**, *29*, 6317–6320), $^2J_{C2,H3ax}$ and $^2J_{C2,H3eq}$ can be used to distinguish between **1**α*p* and **1**β*p* (see ref 34).

(32) Bock, K.; Pedersen, C. *Acta Chem. Scand.* **1977**, *B31*, 354–358.

Scheme 2. Enol Forms of **1**

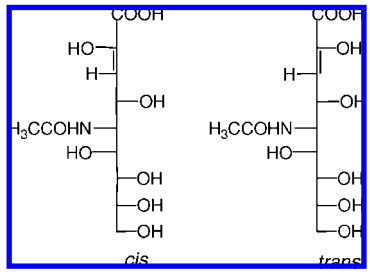

contained intense signals at 40.70 and 39.50 ppm attributed to $C3_{\mathbf{1}\alpha p}$ and $C3_{\mathbf{1}\beta p}$, respectively (data not shown). While additional weaker signals appeared in the same region, they could not be assigned confidently to C3 of **1***k* and **1***h*. However, a moderately strong signal arising from a labeled carbon was observed at 119.85 ppm (Figure 3A) that was tentatively assigned to C3 of **1***e*.

^{1}H-Coupled ^{13}C NMR spectra of [2-^{13}C]**1** and [3-^{13}C]**1** were obtained to measure J_{CH} values involving the putative C2 and C3 carbons of **1***e*. The putative C2 signals appeared as doublets with $J_{CH} = \pm 3.2$ (major signal) and ± 3.4 Hz (minor signal) (Figure 2C), consistent with C2 being coupled to H3 ($^2J_{C2,H3}$) or H4 ($^3J_{C2,H4}$). The putative enol C3 signal was split into a doublet of doublets with $^1J_{C3,H3} = 177.5$ Hz and a longer-range $J_{CH} = \pm 4.7$ Hz (Figure 3B), results consistent with the structure of **1***e*. These data indicate that one of the two possible J_{CH} values involving C2 ($^2J_{C2,H3}$, $^3J_{C2,H4}$) and C3 ($^2J_{C3,H4}$, $^3J_{C3,H5}$) must be small or zero.

Given the low intensities of the putative C2 and C3 enol signals and the possibility of attributing their presence to low-level contaminants, **1** was prepared with contiguous ^{13}C-labeling at C1−C3 to confirm backbone carbon connectivities via $^1J_{CC}$ and $^2J_{CCC}$ values. The ^{13}C NMR spectrum of the trilabeled isotopomer contained C2 and C3 signals at the expected chemical shifts with comparable intensities and with the expected signal multiplicities (Figure 4). Backbone connectivity between C2 and C3 was established from the mutual $^1J_{CC}$ observed in each carbon signal ($^1J_{C2,C3} = 80.6$ Hz). $^1J_{C1,C2} = 76.6$ Hz, as measured at C2, and $^2J_{C1,C3} = \pm 12.4$ Hz, as measured at C3 (sign unknown).[33] The large $^1J_{C2,C3}$ is consistent with one-bond couplings in C=C fragments, and $^1J_{C1,C2}$ is ~10 Hz larger than the corresponding coupling in $\mathbf{1}\alpha p$ and $\mathbf{1}\beta p$ at pH 2.0.[34] The distinctive values of these couplings also allowed an assignment of the weak C1 carbon signal of the enol form at 172.41 ppm (Figure S3). Overall, these results support the conclusion that **1***e* is present in aqueous solutions of **1** at low pH.

J_{CH} values were calculated in enol structural mimics **4** and **5** in their protonated states and with O1′ *anti* to C3 to optimize conjugation of the double bonds (Scheme 3). Calculated $^2J_{C2,H3}$ values in **4** and **5** were similar in magnitude, but the coupling in *cis* enol **4** was negative, while that in *trans* enol **5** was positive. This result suggests that the sign of $^2J_{C2,H3}$ could be used to distinguish between *cis* and *trans* enol configurations. $^1J_{C3,H3}$ is ~10 Hz larger in the *trans* enol (Scheme 3). Calculations of total energies of both structures showed that the *trans* configuration **5** is more stable than **4** by ~3 kcal/mol.

(33) These values differ from those measured in **1***k* ($^1J_{C1,C2} \simeq 65.1$ Hz, $^1J_{C2,C3} \simeq 42.2$ Hz) and for **1***h* (X_2) ($^1J_{C1,C2} = 69.5$ Hz, $^1J_{C2,C3} = 44.0$ Hz).

(34) Klepach, T.; Zhang, W.; Carmichael, I.; Serianni, A. S. *J. Org. Chem.* **2008**, *73*, 4376–4387.

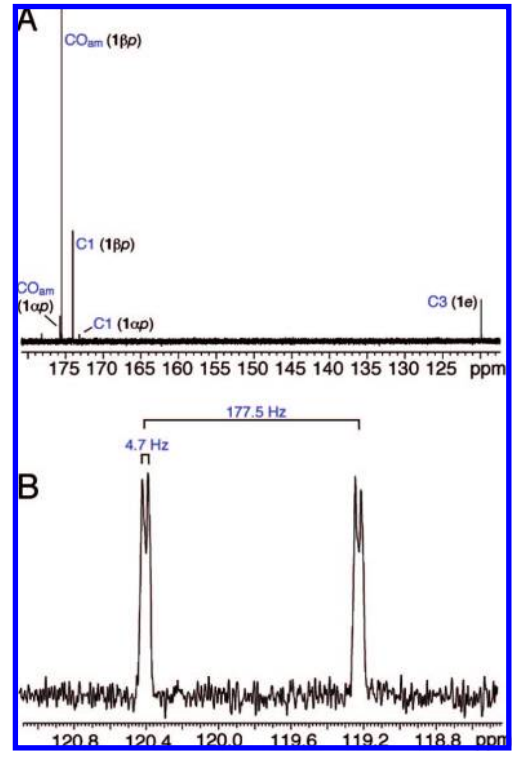

Figure 3. Partial ^{13}C{^{1}H} NMR spectrum of [3-^{13}C]**1** at pH 2.0 and 25 °C. (A) Region showing the natural abundance C1 and amide CO signals of $\mathbf{1}\alpha p$ and $\mathbf{1}\beta p$, and the C3 signal (labeled) of **1***e*. (B) C3 signal of **1***e* in the ^{1}H-coupled ^{13}C spectrum of [3-^{13}C]**1**, showing the $^1J_{CH}$ and longer-range J_{CH} values.

The effects of C1−C2 and C3−C4 bond rotation on calculated J_{CH} values were investigated in simplified enol mimics **6** and **7** (Scheme 4). These structures were geometrically optimized as a function of the C2−C3−C4−C5 torsion angle (90°−270°) in two O1−C1−C2−C3 rotamers (90° and 180°). The latter torsions were chosen to evaluate the effect of double-bond conjugation on the calculated couplings. In most cases, *trans* enol **7** was lower in energy than *cis* enol **6**, although in a few cases the opposite was observed, presumably due to intramolecular H-bonding in **6** that was not present in **7**. $^2J_{C2,H3}$ values showed a significant dependence on the C2−C3−C4−C5 torsion angle (Figure S5B,D), and calculated $^2J_{C2,H3}$ values were similar to those found in **4** and **5** (negative in **6** and positive in **7**). $^2J_{C2,H3}$ values shifted to more negative (less positive) values as the C1−O1 bond (carbonyl) was brought into conjugation with the C2−C3 bond. Calculated $^1J_{C3,H3}$ values shifted to smaller values in the conjugated form of **6**, whereas conjugation increased $^1J_{C3,H3}$ in **7** (Figure S5A,C). $^1J_{C3,H3}$ was uniformly larger in **7** than in **6** in the conjugated structures, whereas $^1J_{C3,H3}$ values were similar in the non-conjugated structures.

Calculated $^3J_{C2,H4}$ values in **6** and **7** were smallest (~2 Hz) in **7**. The experimental $^3J_{C2,H4}$ was predicted to be small or zero (see above). However, it should be noted that the electronegative *N*-acetyl substituent at C5 in **1** (not present in **6** and **7**) may affect this coupling, especially if it orients *anti* to H4. The latter conformation would reduce $^3J_{C2,H4}$ by ~1 Hz, thus rendering it more consistent with the experimental data.

$^1J_{C1,C2}$, $^1J_{C2,C3}$, and $^2J_{C1,C3}$ values were calculated in **6** and **7** as a function of the C2−C3−C4−C5 torsion angle (Figures S6 and S7). Calculated $^1J_{C2,C3}$ values were larger than $^1J_{C1,C2}$ values, in agreement with the experimental observations, although the difference was larger in the calculations.

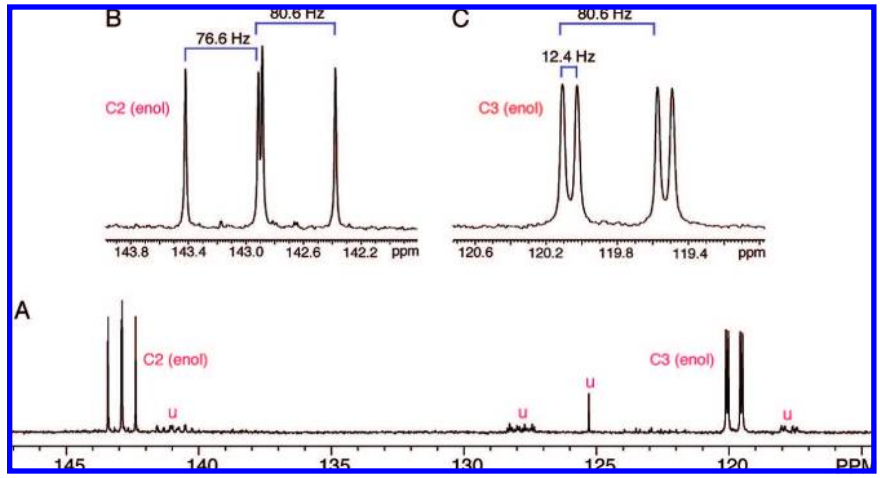

Figure 4. (A) Partial ^{13}C{^{1}H} NMR spectrum of [1,2,3-$^{13}C_3$]**1**, showing the putative C2 and C3 enol signals. Signals labeled "u" were unassigned and possibly arise from other enols. (B,C) Expansions of the C2 and C3 signals in (A), respectively, showing their multiplicities and constituent $^{1}J_{CC}$ and $^{2}J_{CC}$ values.

Scheme 3

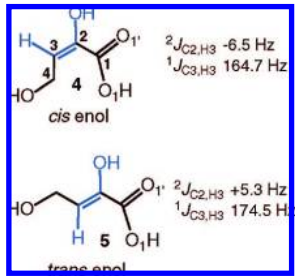

Scheme 4

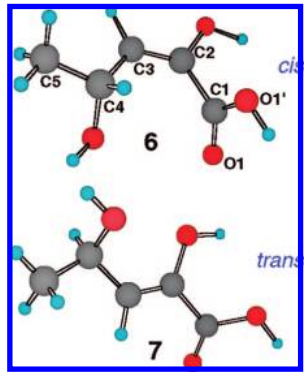

Calculated $^{2}J_{C1,C3}$ values were positive in sign and averaged $\sim +7$ Hz, compared to the experimental value of 12.4 Hz. It should be appreciated, however, that the effect of the C2−O2 bond torsion on these couplings could be appreciable, mediated by O2 lone-pair orbital effects on the C1−C3 molecular fragment. In the present calculations, only one C3−C2−O2−H torsion angle was examined (180°), and presumably appropriate averaging of this torsion that properly mimics behavior in solution would improve the agreement between experiment and theory.[35]

Detection of the putative C2 and C3 enol signals in ^{13}C NMR spectra of [2-^{13}C]**1** and [3-^{13}C]**1**, respectively, depended on solution pH. Signals were observed in spectra obtained on solutions at pH 2.0 but not on the same solutions adjusted to pH 7.0. Enol signal detection could be recovered by adjusting solutions at pH 7.0 back to pH 2.0 with HCl. These results are consistent with those reported for the enol−keto equilibrium of pyruvate, in which the [enol]/[keto] ratio is approximately 100-fold greater for pyruvic acid than for the pyruvate anion. A rationale has been offered for this behavior based on the proposed greater energy gap between keto pyruvate and its enol compared to that for the protonated species.[27]

^{13}C NMR chemical shifts for the enol forms of α-keto acids like **1** have not been well documented in the literature. However, the ^{13}C shifts of propen-2-ol **8** (acetone enol) show C_α at 156.8 ppm and C_β at 95.3 ppm in 2-propanol solvent at 44 °C.[36] These shifts provide a crude calibration for the putative C2 and C3 shifts in **1** and suggest that $C2_{\mathbf{1}e}$ should be downfield of $C3_{\mathbf{1}e}$, as observed experimentally.

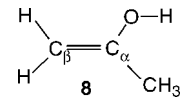

D. pK_a Values of Tautomers of 1. The C2 chemical shifts of **1**α*p*, **1**β*p*, **1***k*, and **1***e* exhibited sufficient pH dependencies to allow estimations of pK_a values for COOH ionization. Titration data (Figure 5) obtained on [2-^{13}C]**1** and fit to a modified form of the Henderson−Hasselbach equation[37] gave the following results: **1**α*p*, 2.5 ± 0.1; **1**β*p*, 2.6 ± 0.1; **1***k*, 2.1 ± 0.1 and 1.8 ± 0.1; **1***e*, 5.5 ± 2.6. The large error in the pK_a of **1***e* results from the lack of data points at the higher pHs of the titration curve (detection of the C2 enol signal is lost at the higher pHs). The true pK_a is expected to be close to 5.5, based on visual inspection of the curve (Figure 5D).

The nearly identical pK_a values for **1**α*p* and **1**β*p* were intermediate in magnitude between those for **1***k* and **1***e*, with **1***k* being most acidic. These results are comparable to those found with pyruvic acid, where pK_a values of the keto and enol forms have been reported to be 1.97 and 3.79, respectively.[27]

(35) DFT calculations on **6**, in which the C1−C2−O2−H and C3−C2−O2−H torsion angles were fixed at 60° and −60°, respectively, gave calculated $^{2}J_{C1,C3}$ values of +8.8 and +9.0 Hz, respectively (C2−C3−C4−C5 torsion fixed at 180°). These results confirm that the effect of the C2−O2 bond torsion on $^{2}J_{CCC}$ values in unsaturated systems mimics that observed in saturated systems (Klepach, T.; Carmichael, I.; Serianni, A. S., unpublished results).

(36) Sojka, S. A.; Poranski, C. F., Jr.; Moniz, W. B. *J. Am. Chem. Soc.* **1975**, *97*, 5953–5955.

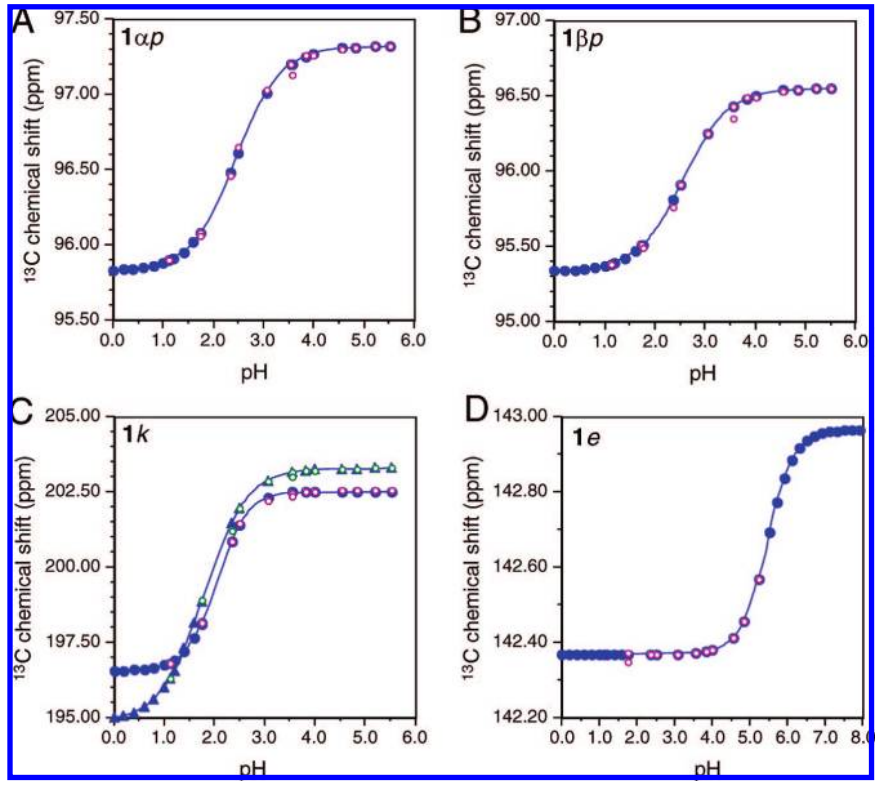

Figure 5. Dependencies of the C2 chemical shifts of **1**α*p* (A), **1**β*p* (B), **1***k* (C), and **1***e* (D) on solution pH. Filled blue circles and blue lines are fits to the experimental data shown in either red or green. Curve fitting gave the pK_a values reported in the text.

It was not possible to estimate the pK_a of the putative hydrate form of **1** since the intensity of signal X_2 decreased rapidly with increasing pH, preventing sufficient digitization of a titration curve.

E. Exchange Rates between Tautomers of 1. ^{13}C Saturation-transfer (ST) experiments[37] were conducted on an aqueous solution of [2-^{13}C]**1** at pH 2.0 and 30 °C to identify species in chemical exchange with the acyclic keto form. Selective irradiation of the C2 signal of **1***k* did not affect the C2 signal intensities of **1**α*p*, **1**β*p*, **1***e*, or **1***h*, suggesting that the unidirectional rate constants for ring-opening, dehydration, and enolization were very small (<0.05 s^{-1}) under these solution conditions. Control ^{13}C ST experiments on aqueous solutions of D-[1-^{13}C]threose at pH 2.0 showed strong reduction of the C1 signals from furanose and hydrate forms upon selective irradiation of C1 of the acyclic aldehydo form, as expected.[38] ST experiments on Neu5Ac at higher temperatures were not conducted to avoid thermal degradation of the sample.

The small unidirectional rate constants of anomerization observed for **1** are consistent with overall rates of anomerization of 3-deoxy-D-*manno*-octulosonic acid (KDO) at pH 7.90 and 25 °C measured by 2D ^{13}C exchange spectrosoopy.[39] Under solution conditions more basic than those used for **1**, which should enhance exchange rates between anomers, furanose−furanose and furanose−pyranose rate constants of 0.02−2.2 s^{-1} were determined, but rate constants for pyranose−pyranose exchange were estimated at less than 0.01 s^{-1}.

F. Solvent Deuterium Exchange in 1. Given the relatively high abundance of enol forms of **1** in aqueous solution, ^{1}H NMR studies were conducted on unlabeled **1** in ^2H_2O solvent at p^{2}H 8.0 to investigate solvent deuterium exchange at C3. The $H3_{ax}$ and $H3_{eq}$ signals in **1**α*p* and **1**β*p* in ^1H_2O solvent at pH 8.0 were assigned (Figure 6A) on the basis of the relative magnitudes of $^3J_{H3ax,H4}$ and $^3J_{H3eq,H4}$.

Solvent deuterium exchange was very rapid at p^{2}H 8.0 and 25 °C (Figure 6B), with virtually full and selective exchange observed at $H3_{ax}$ after 47 min. ^{1}H NMR data obtained after incubation of the same reaction mixture for 6 days were identical to those obtained after 47 min (spectrum not shown). These results are consistent with solvent deuterium exchange properties for **1** reported previously by Schmidt and Friebolin.[40]

The facile and selective exchange of $H3_{ax}$ in **1**α*p* and **1**β*p* presumably occurs via the acyclic keto form **1***k*. If so, **1***k* probably assumes a relatively stable pseudo-cyclic conformation in solution, containing relatively distinct and persistent C3−$H3_{ax}$ and C3−$H3_{eq}$ bonds to account for the observed exchange selectivity. The possibility of ^{1}H/^{2}H exchange via cyclic structures was eliminated through studies of 2-*O*-methyl-β-D-*N*-acetyl-neuraminic acid (**2**). In contrast to **1**, solvent deuterium

(37) The following equation was used to fit the NMR chemical shift data: $\delta(\mathrm{pH}) = [\delta_{base} + \delta_{acid} \times 10^{n(pK_a-pH)}]/[1 + 10^{n(pK_a-pH)}]$, where δ_{acid} and δ_{base} are the chemical shifts at the acid and base plateaus and n is the Hill coefficient. Parameters δ_{base}, δ_{acid}, pK_a, and n were optimized simultaneously during the data fit using the Solver Routine in Microsoft Excel.

(38) Serianni, A. S.; Pierce, J.; Huang, S.-G.; Barker, R. *J. Am. Chem. Soc.* **1982**, *104*, 4037.

(39) Fesik, S. W.; Kohlbrenner, W. E.; Gampe, Jr., R. T.; Olejniczak, E. T. *Carbohydr. Res.* **1986**, *153*, 136–140.

(40) Schmidt, H.; Friebolin, H. *J. Carbohydr. Chem.* **1983**, *2*, 405–413.

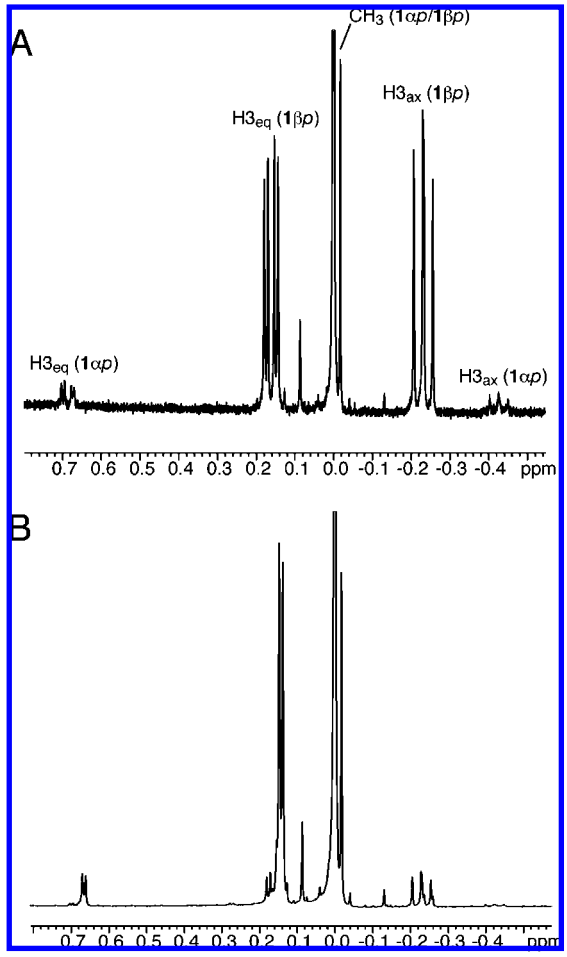

Figure 6. Partial ^{1}H NMR spectrum (600 MHz) of **1** immediately after dissolution in $^{2}H_2O$ (A) and after incubation at 25 °C for 150 h (B). Signals from $H3_{ax}$ in **1**α*p* and **1**β*p* are nearly absent, whereas those from $H3_{eq}$ (doublets) remain observable.

exchange was not observed in **2** at either $H3_{ax}$ or $H3_{eq}$ after 21 days at p^{2}H 12.0 and 25 °C.

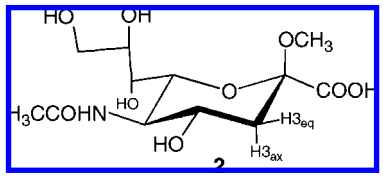

Conclusions

Aqueous solutions of *N*-acetyl-neuraminic acid (**1**) contain mainly the β-pyranose form, with the α-pyranose second in abundance. In addition to these cyclic forms, three acyclic forms were detected at low levels (0.5−1.9% at pH 2). These acyclic forms are difficult to observe by ^{13}C NMR spectroscopy at natural abundance, but detection and quantification are greatly improved when measurements are made with ^{13}C-labeled samples, especially those singly labeled at C2. Prior studies have utilized ^{13}C-labeling of **1** and its homopolymers (e.g., polysialic acid, PSA) to investigate the anomeric specificity of CMP-*N*-acetyl-neuraminic acid synthetase[41] and PSA structure *in vitro* and *in vivo* (*E. coli*).[42]

The characteristic C2 chemical shift of the keto form of **1** makes its detection and quantification relatively straightforward, whereas the presence of hydrate and enol forms is not easily

Scheme 5. Potential Lactones of **1** (Keto, Keto Hydrate, and Enol Forms)

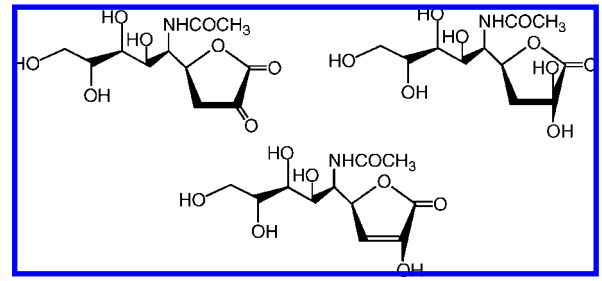

confirmed. The latter problem is caused by the relatively limited literature on ^{13}C chemical shifts of these forms and the underlying concern that weak signals observed in ^{13}C NMR spectra may be due to low-level contaminants present in the sample.

The observation of weak C2 signals in the ^{13}C NMR spectrum of [2-^{13}C]**1**, consistent with the presence of enol forms, was followed up by studies of the [3-^{13}C] and [1,2,3-$^{13}C_3$] isotopomers. The data, when taken collectively, strongly support the presence of detectable levels of Neu5Ac enol in solution. While the predominant configuration could not be determined experimentally, DFT calculations suggest that the *trans* form is probably preferred. DFT calculations also predict that the *cis* and *trans* enol configurations can be distinguished on the basis of the different signs of $^{2}J_{C2,H3}$ in their structures. This may prove useful in future structural characterization of these and related species.

Of the three acyclic monomeric forms of Neu5Ac, confirmation of the presence of the keto hydrate proved most challenging, and the present data cannot be considered unequivocal. However, when the present data are viewed collectively, a likely C2 hydrate signal emerges (X_2).

Exploitation of the pH dependencies of C2 chemical shifts yielded pK_a values for the cyclic, keto, and enol forms of Neu5Ac. The enol form is least acidic, and it is assumed that the ionization being measured is that of the COOH group, and not the enol C2 OH. Presumably, raising the pH above 6−7, where the abundance of the enol form decays, results in the ionization of the C2 hydroxyl, thus destabilizing the enol due to the presence of two negative charges in close proximity.

Particularly striking about the ^{13}C NMR spectra of ^{13}C-labeled Neu5Ac was the presence of weak but reproducible signals that could not be attributed to the expected cyclic and acyclic monomeric forms of the molecule. This observation contrasts with prior studies of ^{13}C-labeled aldopentoses[8] and aldohexoses,[9] where essentially all signals arising from labeled species could be assigned to monomeric forms. An identification of these unknown Neu5Ac species was not attempted, but it is noted that Neu5Ac lactonization can potentially occur in aqueous solution, especially at low pH, giving the structures shown in Scheme 5. These species may account for the additional keto, enol, and hydrate signals observed in ^{13}C NMR spectra of ^{13}C-labeled Neu5Ac. In addition to monomeric lactones, intermolecular dimerization and oligomerization (esterification) involving the COOH and OH functionalities in different Neu5Ac

(41) Ambrose, M. G.; Freese, S. J.; Reinhold, M. S.; Warner, T. G.; Vann, W. F. *Biochemistry* **1992**, *31*, 775–780.
(42) Azurmendi, H. F.; Vionnet, J.; Wrightson, L.; Trinh, L. B.; Shiloach, J.; Freedberg, D. I. *Proc. Natl. Acad. Sci. U.S.A.* **2007**, *104*, 11557–11561.

molecules may also contribute to these weak signals, with their relative intensities dependent on Neu5Ac concentration.

Solvated DFT calculations conducted on structural mimics of **1***h* and **1***e* have provided additional information on which to base signal assignments. These calculations, however, involve inherent structural assumptions that were not fully explored, especially those regarding the preferred conformations of these acyclic species in solution.[43] Related to this limitation is the fact that Neu5Ac undergoes facile solvent deuterium exchange in aqueous solution, and this exchange occurs more rapidly at the axial H3 in both **1**αp and **1**βp. This exchange correlates with the relatively high abundance of the keto form in solution. The observed exchange selectivity implies that the acyclic keto form probably retains some cyclic character in solution, possibly assuming a pseudo-cyclic conformation in which $H3_{ax}$ and $H3_{eq}$ retain orientations similar to those found in the cyclic pyranoses.

The fact that solutions of Neu5Ac contain acyclic keto, hydrate, and enol forms may have implications for its biological functions. At low pH uncharacteristic of most biological environments, the enol and hydrate forms are relatively abundant in aqueous solution. However, as the pH approaches the physiological value of ~7.0, these forms decrease substantially, thus reducing (but not necessarily eliminating) the likelihood of their participation as substrates in enzyme-catalyzed reactions. However, in subcellular regions of low pH (e.g., lysosomes) or in the low-pH environment of the stomach, these forms are more prevalent. The extent to which these solution behaviors influence Neu5Ac biological functions remains to be explored.

Acknowledgment. This work was supported by a grant from the National Institutes of Health (GM059239, A.S.). The Notre Dame Radiation Laboratory is supported by the Office of Basic Energy Sciences of the United States Department of Energy. This is Document No. NDRL-4742 from the Notre Dame Radiation Laboratory. The authors thank Omicron Biochemicals, Inc. for the generous gift of the ^{13}C-labeled Neu5Ac isotopomers.

Supporting Information Available: Scheme S1, projections for $^2J_{C2,H3R/S}$ in **1***h* conformers and predicted couplings; Figure S1, $^{13}C\{^1H\}$ NMR spectra of pyruvic acid and sodium pyruvate; Figure S2, effect of the C2−C3−C4−C5 torsion angle in **3** on calculated total energies and $^2J_{C2,H3R/S}$ and $^1J_{CC}$ values; Figure S3, C1 signals of **1**αp, **1***e*, and X_1 in the partial $^{13}C\{^1H\}$ NMR spectrum of [1,2,3-$^{13}C_3$]**1**; Figure S4, C2 signals of **1**αp, **1**βp, and X_1 in the partial $^{13}C\{^1H\}$ NMR spectrum of [1,2,3-$^{13}C_3$]**1**; Figure S5, effect of the C2−C3−C4−C5 torsion angle on calculated J_{CH} in **6** and **7**; Figure S6, effect of the C2−C3−C4−C5 torsion angle on calculated $^1J_{CC}$ in **6** and **7**; Figure S7, effect of the C2−C3−C4−C5 torsion angle on calculated $^2J_{C1,C3}$ in **6** and **7**; and complete ref 12. This material is available free of charge via the Internet at http://pubs.acs.org.

JA077565G

(43) Larger disparities between calculated and experimental *J*-couplings are not considered to arise from inherent limitations of the DFT methodology but rather from simplifications and assumptions in the structural models used to calculate the couplings. In saccharides, the latter often involve the conformational properties of exocyclic OH groups, which can exert a major effect on both J_{CH} and J_{CC} values. Density functional theory with the B3LYP functional is known to produce accurate structural and energetic parameters in most organic molecules. This particular functional is specifically parametrized to reproduce accurate thermochemistry and matches closely results from high-level composite methods such as the *Gaussian*03 approach. Work in this laboratory and by other investigators has shown high agreement between B3LYP predictions of indirect nuclear spin−spin coupling constants and calculated couplings obtained by accurate high-level coupled-cluster-based calculations. When structural models that closely mimic behavior in solution are available, ^2J and ^3J values (C−H and C−C) calculated by DFT are usually within 0.2−0.4 Hz of the experimental values. In general, absolute errors in calculated couplings are 5−6% (underestimated) for J_{CH} and 5−10% (overestimated) for J_{CC} (Cloran, F.; Carmichael, I.; Serianni, A. S. *J. Phys. Chem. A* **1999**, *103*, 3783–3795).